4-2008

Roles of FGFR3 During Morphogenesis of Meckel's Cartilage and Mandibular Bones

Bruce A. Havens
University of Connecticut School of Medicine and Dentistry

Dimitris Velonis
University of Connecticut School of Medicine and Dentistry

Mark S. Kronenberg
University of Connecticut School of Medicine and Dentistry

Alex C. Lichtler
University of Connecticut School of Medicine and Dentistry

Bonnie Oliver
University of Connecticut School of Medicine and Dentistry

See next page for additional authors

Published in final edited form as:
Dev Biol. 2008 April 15; 316(2): 336–349.

Roles of FGFR3 during morphogenesis of Meckel's cartilage and mandibular bones

Bruce A. Havens[a], **Dimitris Velonis**[a], **Mark S. Kronenberg**[b], **Alex C. Lichtler**[b], **Bonnie Oliver**[c], and **Mina Mina**[a,*]

a*Department of Craniofacial Sciences, School of Dental Medicine, University of Connecticut Health Center, Farmington, CT, 06030, USA*

b*Department of Genetics and Developmental Biology, School of Medicine, University of Connecticut Health Center, Farmington, CT 06030, USA*

c*Department of Reconstructive Science, School of Dental Medicine, University of Connecticut Health Center, Farmington, CT, 06030, USA*

Abstract

To address the functions of FGFR2 and FGFR3 signaling during mandibular skeletogenesis, we over-expressed in the developing chick mandible, replication-competent retroviruses carrying truncated FGFR2c or FGFR3c that function as dominant negative receptors (RCAS-dnFGFR2 and RCAS-dnFGFR3). Injection of RCAS-dnFGFR3 between HH15−20 led to reduced proliferation, increased apoptosis, and decreased differentiation of chondroblasts in Meckel's cartilage. These changes resulted in the formation of a hypoplastic mandibular process and truncated Meckel's cartilage. This treatment also affected the proliferation and survival of osteoprogenitor cells in osteogenic condensations, leading to the absence of five mandibular bones on the injected side. Injection of RCAS-dnFGFR2 between HH15−20 or RCAS-dnFGFR3 at HH26 did not affect the morphogenesis of Meckel's cartilage but resulted in truncations of the mandibular bones. RCAS-dnFGFR3 affected the proliferation and survival of the cells within the periosteum and osteoblasts. Together these results demonstrate that FGFR3 signaling is required for the elongation of Meckel's cartilage and FGFR2 and FGFR3 have roles during intramembranous ossification of mandibular bones.

Introduction

The development of the mandible is a dynamic multi-step process that starts with the formation of mandibular processes from the first branchial arch. At the time of their formation, the mandibular processes consist of mesenchyme encased by epithelium derived from ectoderm and endoderm. The skeletal elements in the mandibular arch are made by cranial neural crest cells (NCC) (reviewed by Chai and Maxson, 2006; Le Douarin et al., 2004; Santagati and Rijli, 2003). Although NCCs provide species-specific patterning information in the developing branchial arch skeleton (Schneider and Helms, 2003; Tucker and Lumsden, 2004), the fate and differentiation of NCCs populating the branchial arches are determined by signaling interactions with the surrounding tissues, including the endoderm of the foregut and the

* Address correspondence to: Mina Mina Division of Pediatric Dentistry Department of Craniofacial Sciences UConn Health Center Farmington, CT 06030 Telephone: (860) 679−4081 Fax: (860) 679−4078 E-mail: Mina@nso1.uchc.edu.

epithelium (reviewed by Chai and Maxson, 2006; Le Douarin et al., 2004; Santagati and Rijli, 2003).

Candidate signaling molecules involved in the morphogenesis of the mandibular processes include members of the fibroblast growth factor family (FGFs), bone morphogenetic factors (BMPs), transforming growth factors (TGFs), members of the wingless family (WNTs) and Sonic hedgehog (Shh) (reviewed by Chai and Maxson, 2006Francis-West et al., 2003; Mina, 2001; Richman and Lee, 2003; Santagati and Rijli, 2003; Tapadia et al., 2005).

FGFs represent a family of conserved signaling molecules that have been implicated in various aspects of vertebrate craniofacial development (reviewed by Ellsworth et al., 2002; Nie et al., 2006; Ornitz, 2005; Ornitz and Marie, 2002). Several FGF and FGF receptors are expressed in the mandibular epithelium and mesenchyme (reviewed by Nie et al., 2006). The consequences of perturbations in components of FGF/FGFR signaling have revealed essential roles of FGF signaling in several aspects of mandibular morphogenesis, including mediating growth-promoting epithelial-mesenchymal interactions, formation of pharyngeal pouches, and survival of mandibular mesenchyme (reviewed by Nie et al., 2006).

Loss-of-function analysis of FGF8 provided clear evidence for its involvement in mandibular morphogenesis. Deletion of *Fgf8* from the mandibular epithelium (Trumpp et al., 1999) and decreased dosage of FGF8 in mice containing hypomorphic alleles of *Fgf8* (Abu-Issa et al., 2002; Frank et al., 2002; Macatee et al., 2003) resulted in formation of a smaller mandible, extensive apoptosis in mandibular mesenchyme, and loss of skeletal elements in the caudal region of the mandible including the jaw articulation. Studies in zebrafish provided further evidence for the roles of FGF signaling in the formation and patterning of pharyngeal pouches and cartilages in the branchial arches (Crump et al., 2004a; Crump et al., 2004b; David et al., 2002; Nissen et al., 2003; Trokovic et al., 2003; Walshe and Mason, 2003). Studies in chick embryos showed roles of FGF signaling in various aspects of mandibular morphogenesis including the survival of mesenchyme (Wilson and Tucker, 2004), in mediating epithelial-mesenchymal interactions regulating the outgrowth of the mandibular mesenchyme and elongation of Meckel's cartilage (Mina et al., 2002; Richman et al., 1997), and in chondrogenesis of micromass cultures derived from mandibular mesenchyme (Bobick and Kulyk, 2006; Bobick et al., 2007; Mina et al., 2002). Although these results indicate essential roles of FGF signaling in mandibular morphogenesis, there remain questions regarding which of the FGFRs are involved in the skeletogenic differentiation of the NCC-derived mandibular mesenchyme.

Development of the chick mandibular processes presents an excellent experimental system to gain further insight into roles of FGF/FGFR signaling in skeletogenesis of NCC-derived mandibular mesenchyme. In the chick embryo, the mandibular processes are recognizable at HH15 (E2.5). The formation of Meckel's cartilage starts with the chondrogenic condensations at around HH25/26 (E5). Later at around HH28 (E6) cells within the chondrogenic condensations differentiate into chondrocytes and begin synthesis and secretion of cartilage-specific extracellular matrix proteins, such as aggrecan and type II collagen. Chondrogenic differentiation in the developing mandible occurs in a caudal to rostral gradient, i.e. it begins in the caudal region and later extends into the more rostral region (Miyake et al., 1996; Mina et al., 2007).

The chick mandible contains six bones (angular, supra-angular, articular, splenial, dentary, and mentomandibular) that are formed in a caudal to rostral gradient by intramembranous ossification (Mina et al., 2007). The formation of the osteogenic condensations occurs at around HH31 (E7−7.5) and mineralization of the mandibular bones at HH34 (E8). By HH36 (E10),

the mandibular processes contain a fully differentiated Meckel's cartilage surrounded by six mandibular bones (Mina et al., 2007).

The prominent expression of *Fgfr2* and *Fgfr3* in osteogenic and chondrogenic tissue suggests essential functions for these receptors during chondrogenesis and osteogenesis in the mandibular arch. *Fgfr2* and *Fgfr3* are expressed throughout all phases of chick mandibular skeletogenesis (Havens et al., 2006; Mina et al., 2002; Wilke et al., 1997). Initially, these receptors are expressed in mesenchymal condensations giving rise to Meckel's cartilage and various bones. Later, *Fgfr2* and *Fgfr3* are expressed in the differentiating Meckel's cartilage and in the osteoblasts and periosteal tissues of the mandibular bones (Supplemental Fig. 1).

To address the functions of FGFR2 and FGFR3 signaling during mandibular skeletogenesis, we over-expressed in the developing chick mandible, replication-competent retroviruses carrying truncated FGFR2c or FGFR3c that function as dominant negative receptors (RCAS-dnFGFR2 and RCAS-dnFGFR3). Our results demonstrate that FGFR3 signaling is required for the elongation of Meckel's cartilage, and FGFR2 and FGFR3 have roles during intramembranous ossification of mandibular bones.

Materials and Methods

Viral constructs and stocks

The dominant-negative FGFR3c construct (RCAS-dnFGFR3) encoding aa 1−401 and containing a carboxy-terminal c-myc epitope tag was constructed by deletion of sequences past the transmembrane domain as described (Velonis et al., 2004). A viral construct containing a kinase deleted form of chick FGFR2c (RCAS-dnFGFR2) encoding aa 1−475 with a carboxy-terminal hemagglutinin (HA) epitope tag (Ratisoontorn et al., 2003) was kindly provided by Dr. Hyun-Duck Nah. A viral construct containing the coding sequence of green fluorescent protein (GFP) (RCAS-GFP) was used as a control (Erceg et al., 2003). Retroviral titers of about 10^9 pfu/ml were prepared from a chick embryonic fibroblast cell line (DF-1) infected with various retrovirus vectors as described (Ferrari et al., 1999; Morgan and Fekete, 1996) and used for all experiments.

Antibodies

AMV-3C2 antibody (Developmental Studies Hybridoma Bank) that recognizes retroviral Gag protein p19 was used to visualize cells infected with RCAS virus (Potts et al., 1987). Mouse monoclonal anti-myc (9E10, Sigma) was used to detect expression of myc-tagged dnFGFR3 protein. Mouse monoclonal anti-HA antibodies (HA.11, Covance; F-7, Santa Cruz Biotechnology) were used to detect expression of HA-tagged dnFGFR2 protein by immunohistochemistry and Western blot analysis respectively. A rabbit polyclonal anti-phosphorylated histone 3 (H3-p) antibody (Ser10, Upstate Biotechnologies) was used to identify mitotic cells (Hendzel et al., 1997).

Western blot analysis

DF-1 cells were infected with 10^6 cfu/ml of the different viral constructs and cultured for four days. Cell lysates and Western blot analysis were performed as previously described with minor modifications (Oliver et al., 1994). Lysates containing equivalent protein (40 μg) were mixed with SDS-PAGE loading buffer, resolved on 12% SDS-PAGE, and electro-transferred to Immobilon-P membranes (Millipore Corp). Membranes were incubated for 2 hours with anti-myc, or anti-HA antibodies at a concentration of 10 μg/ml, and then for 30 min with a 1:10,000 dilution of horseradish-peroxidase linked anti-mouse secondary antibody (Amersham). Immunoblots were developed using enhanced chemiluminescence (Amersham).

Mitogenic assay

DF-1 cells were infected for one week with 10^6 pfu/ml of various viral constructs. The efficiency of the infection was examined by immunocytochemistry using anti-myc (1:2000 dilution) and anti-HA (1:2500 dilution) antibodies. Infected cultures were then re-plated at a density of 3×10^5 cells in 35 mm dishes in DMEM medium containing 10% FBS. After 24 hrs, cultures were changed to medium containing 1% FBS and then grown in the presence or absence of 20 ng/ml FGF2 (R&D Systems) and 10 μg/ml heparin (Sigma). After 48 hrs, attached cells were harvested with trypsin/EDTA and counted with a Coulter Counter. For each construct, the percent increase in the number of attached cells in response to FGF2 was determined relative to that in cells grown in the absence of FGF2. Values represent the mean ± SE from duplicated cultures in at least two independent experiments.

Tissue fixation and processing

Tissue fragments were fixed in freshly prepared 4% paraformaldehyde in PBS at 4°C overnight, and micromass cultures were fixed in 4% paraformaldehyde for 10 min and scraped from the culture dishes. All fixed tissues were dehydrated and processed for paraffin embedding. Seven μm sections were mounted on Probe-On Plus slides and processed for various analyses.

Immunohistochemistry

Immunohistochemistry was performed on paraffin embedded sections. Sections were quenched in 1% H_2O_2 and incubated with Target Retrieval Solution (DakoCytomation) for 20 min at 95°C. Slides were incubated with blocking solution and then with primary antibodies (AMV-3C2: 1/100, 9E10: 1/4000, HA.11: 1/1000, Ser10: 1/1000) overnight at 4°C. Slides were rinsed and incubated for 30 min at room temperature with a 1:200 dilution of secondary biotinylated horse-anti-mouse or goat-anti-rabbit antibodies followed by a 30 min incubation with avidin-biotinylated horseradish peroxidase (Vector Labs). 3−3'-Diaminobenzidine (DAB Substrate Kit, Vector Labs) was used as the substrate for horseradish peroxidase.

Chicken embryos and microinjections

Fertilized pathogen-free white leghorn chick eggs (SPAFAS; Charles River Laboratories) were incubated at 37.5°C in a humidified incubator and embryos were staged according to Hamburger and Hamilton (HH) (Hamburger and Hamilton, 1951). At desired stages of development (HH15−26, embryonic days E2.5-E5), eggs were windowed and the right side of the face or right forelimb was exposed by removing the vitelline membrane. Concentrated virus was thawed and mixed with 4% (v/v) fast green as a tracer dye to visualize the region of microinjection. Injections were performed using pulled glass capillary pipettes attached to a Narishinge microinjector. After injection, 1−2 drops of antibiotic/antimycotic were added on top of the membrane, eggs were sealed and returned to the incubator for various times (Morgan and Fekete, 1996).

Skeletal whole-mount staining and analysis

Embryos were processed for staining with Alcian blue and alizarin red as previously described (Wang et al., 1998).

In situ hybridization to whole-mounts and sections

Whole-mount hybridization using digoxigenin-labeled RNA probes and hybridization to tissue sections using ^{32}P-labeled antisense RNA probes were performed as previously described (Mina et al., 2002). The cDNAs for this study included *Fgfr2* and *Fgfr3* (Mina et al., 2002), *Sox9* (Healy et al., 1999), *dHand* (Srivastava et al., 1995), *Barx1* (Barlow et al., 1999), *Dlx5* (Ferrari et al., 1999), *Msx1* (Mina et al., 1995), *PTH-1R* (Vortkamp et al., 1996), *Runx2*

(Stricker et al., 2002), *Osteocalcin* (Neugebauer et al., 1995) and *aggrecan core protein* (Mina et al., 2007). Individuals who kindly provided these cDNAs include Drs. C. Healy (*Sox9*), D. Srivastava *(dHand)*, P. Francis-West *(Barx1)*, R. Kosher *(Dlx5)*, C. Tabin (*PTH-1R*), S. Sticker (*Runx2*), L. Gerstenfeld (*Osteocalcin*), and M. Tanzer (*aggrecan*). Following *in situ* hybridization, the sections were stained with hematoxylin or toluidine blue and mounted with Permount. Using Adobe Photoshop 7.0 software, the silver grains in the dark-field image were selected, colored red, and then superimposed onto the bright-field images.

Cell proliferation and apoptosis assays

For analysis of cell proliferation, mandibles were fixed two to six days after injection and subjected to immunohistochemistry with an H3-p antibody as described above. An *in Situ* Cell Death Detection Kit (Roche) was used to detect apoptotic cells in sections adjacent to those used for analysis of cell proliferation in each mandible. For quantitative analysis, equivalently defined areas on the injected and uninjected sides were outlined and measured using ImageJ software. Defined areas after injection between HH17−20, included the entire area of the mandibular mesenchyme at day two (8−12 sections), the area of newly formed Meckel's cartilage (defined by Alcian blue staining and morphological criteria) at day three (6 sections), different regions of differentiated Meckel's cartilage at day four (rostral, middle and caudal third) (10−12 longitudinal and 13−15 cross sections), and the condensation for the supra-angular bone at day four as defined by proximity to the caudal region of Meckel's cartilage (8−17 sections). The cell proliferation and apoptosis in differentiated angular bone was measured in 8−13 sections six days after injection at HH26. In each defined area, H3-p positive and TUNEL-positive cells were individually counted using ImageJ. Values for cell proliferation and apoptosis represent the mean ± SE of positively stained cells/mm^2 that were determined from 6−17 sections (described above) from at least four different embryos at each time point.

Micromass cultures and analyses

Micromass cultures were prepared from the mandibular mesenchyme of HH23 pathogen-free chick embryos as previously described (Mina et al., 1991). Infection of micromass cultures was carried out as previously described (Lizarraga et al., 2002) with some modifications. Briefly, before plating, dissociated cells (1.5×10^7 cells/ml) were incubated in medium with 10% fetal calf serum containing 2.5×10^9 pfu/ml of various viruses at 37°C for 2 hours. The cells were then plated as 20 μl spots in the center of 4 well plates. After 2 hours, media containing a 60:40 ratio of F12:DMEM, 2% fetal calf serum, 2 mM glutamine, 200 μg/ml ascorbic acid, 100 units/ml penicillin, 100 μg/ml streptomycin, 0.25 μg/ml fungizone and 10^8 pfu/ml of viruses was added. The accumulation of cartilage matrix was monitored histochemically by staining with Alcian blue (Mina et al., 1991), and was quantified after extraction of Alcian blue spectrophotometrically using an ELISA reader with a 630nm filter (Hassell and Horigan, 1982; Meyer et al., 2001). Histochemical staining for Peanut agglutinin (PNA), was performed as previously described (Gehris et al., 1997) with 100 μg/ml peroxidase-conjugated PNA (Sigma) and a DAB substrate kit (Vector Laboratories). The areas of cultures stained with PNA and Alcian blue were quantified using the Color Range and Histogram commands in Adobe Photoshop (version 7.0) on images acquired under identical exposure and lighting conditions. To determine the ratio of PNA to Alcian blue staining in each culture, PNA stained cultures were restained with Alcian blue. Values for all micromass experiments represent mean ± SE determined from triplicate cultures in at least two independent experiments.

Statistical analysis

Unpaired, two-tailed t tests were performed to determine statistically significance differences and $p < 0.01$ was considered statistically significant.

Results

Characterization of dominant negative FGFR3 construct *in vitro*

Western blot analysis of DF-1 cells infected with RCAS-dnFGFR3 using anti-myc antibody showed the presence of an intact protein product of approximately 82kDa (Supplemental Fig. 2A). Antibody staining showed the expression of myc-tagged protein in greater than 80% of the DF-1 cells infected for 4 days with RCAS-dnFGFR3 (data not shown).

To assess the efficiency of dnFGFR3 in blocking signal transduction, its ability to inhibit the mitogenic response of DF-1 cells to FGF2 was examined. FGF2 induced increases in the number of cells in cultures of uninfected cells and cells infected with control virus (Supplemental Fig. 2C). In cultures infected with RCAS-dnFGFR3, FGF2 treatment resulted in a markedly reduced mitogenic response (Supplemental Fig. 2C) indicating that this construct acts as a dominant-negative receptor.

dnFGFR3 affected mandibular morphogenesis

To assess the effects of blocking FGFR3 signaling on mandibular morphogenesis, RCAS-dnFGFR3 or control viruses were injected into the right half of the mandible of chick embryos at early (between HH15−20) and later (HH 26) stages of development.

We first examined the onset and the extent of viral infection and the expression of dnFGFR3 in the developing mandible. In embryos injected at early stages of development, expression of viral Gag and myc-tagged dnFGFR3 was detected in the injected side in a high percentage of the cells at one day and in the majority of cells at two days (Fig. 3B). At one and two days post-injection, Gag expression was detected at higher levels and in a higher percentage of cells including the chondrogenic mesenchyme as compared to myc-tagged dnFGFR3 (data not shown). At 4 days, Gag and dnFGFR3 were expressed in the mandibular epithelium and most of the mandibular mesenchyme including the chondrocytes of Meckel's cartilage, osteogenic condensations and muscles of the tongue (Supplementary Figs. 3A-C and data not shown). At 4 days after injection at later stages of development, expression of Gag and myc-tagged dnFGFR3 were detected in most of the undifferentiated mandibular mesenchyme, small clusters of chondrocytes in Meckel's cartilage, and the majority (but not all) of the osteoblasts in the mandibular bones in the injected side (data not shown). Thus, injections at early stages resulted in widespread infection throughout the injected side of mandible, whereas injection at later stages resulted in more localized and limited infections.

Next we examined the effects of dnFGFR3 during mandibular morphogenesis. We have recently reported that injection of dnFGFR3 resulted in stage and region specific abnormalities in the outgrowth of the developing mandible, morphogenesis of the Meckel's cartilage and mandibular bones (Mina et al., 2007). Injection between HH17−20 led to severe defects in mandibular outgrowth (Figs. 1B & 2A), a high frequency of truncation of the rostral end and shortening of Meckel's cartilage (83%, n=6, Fig 1B), and high frequency of absence of five of the mandibular bones (Fig. 1B & Table 1). We also noted alterations in the position and shape of the elements in the articulating end of the Meckel's cartilage on the injected side (Fig. 1B). Injections of either RCAS-dnFGFR3 or control viruses at HH15 resulted in a low survival rate. Surviving embryos injected with RCAS-dnFGFR3 displayed defects in mandibular outgrowth similar to those after injection at HH17−20 (data not shown). Injection at later stages did not affect the morphogenesis of Meckel's cartilage (Fig. 1C), caused only mild defects in mandibular outgrowth in a small percentage of embryos (Mina et al., 2007), and led to the formation of five smaller than normal mandibular bones (Figs. 1C, D and Table 1). Mandibular morphogenesis on the injected side of the embryos injected with control viruses (n=24) was

indistinguishable from the uninjected side (Fig. 1A), indicating that virus injection itself does not disturb mandibular morphogenesis.

As injections of RCAS-dnFGFR3 between HH17−20 had high survival rates and displayed the most consistent and severe abnormalities in the outgrowth of the mandibular process and Meckel's cartilage, further characterization of the underlying mechanisms leading to these abnormalities in Meckel's cartilage was investigated in this group.

dnFGFR3 did not affect the early patterning of the developing mandible

The earliest detectable defects in the growth of the mandibular processes after injection at early stages were noted three days after injections (Fig. 2B), suggesting that defects are related to alterations in expression of components of signaling pathways regulating mandibular outgrowth.

To investigate this possibility we examined the expression of a selected number of transcription factors known to be downstream of signaling pathways regulating mandibular patterning. However, whole mount *in situ* hybridization revealed no noticeable changes in the intensity and domain of expression of these transcription factors on the injected sides compared to the uninjected sides at 2 and 3 days after injections (Figs. 2D-G and data not shown). These results show that defects in mandibular outgrowth are not related to compromised integrity of the NCC population in the mandibular mesenchyme, nor to alterations in early signaling activities regulating mandibular outgrowth.

dnFGFR3 affected cell survival, proliferation and differentiation during chondrogenesis of Meckel's cartilage

The unchanged patterns of expression of regulatory genes in the treated side suggested that the truncation of the developing mandible may be related to the abnormality in Meckel's cartilage that in turn regulates mandibular outgrowth. Thus, we next studied the effects of dnFGFR3 on the formation and morphogenesis of Meckel's cartilage by examining the patterns of expression of markers of early (*Sox9)* and late (*Aggrecan*) stages of chondrogenesis, and changes in apoptosis and cell proliferation in the injected and uninjected sides.

At two days after injection, at the time of the formation of chondrogenic condensations, there were noticeable decreases in the domain and intensity of expression of *Sox9* on the injected sides (Figs. 3A & 3B), indicating that dnFGFR3 led to the formation of a smaller chondrogenic condensation. Analysis of cell proliferation showed no differences in the number and distribution of proliferating cells in the mandibular mesenchyme in the injected and uninjected sides (Table 2). In contrast, TUNEL analysis showed a two fold increase in the number of apoptotic cells in the mesenchyme on the injected side (Table 2). Apoptotic cells were detected in the area of the chondrogenic condensation (Fig. 4A) suggesting that the formation of smaller *Sox9*-expressing chondrogenic condensation was related to increased apoptosis.

Analysis at three days after injection (after the onset of chondrogenesis and during the elongation of Meckel's cartilage) showed marked region-specific changes in expression of *Sox9* and *aggrecan* along the caudal-rostral axis of Meckel's cartilage on the injected side (Figs. 3C-M). The middle and rostral/growing ends of the newly formed Meckel's cartilage on the injected side showed noticeable changes in the domain and intensity of *Sox9* and *aggrecan* expression (Figs. 3H-M). On the other hand, the patterns of *aggrecan* and *Sox9* expression in the caudal region were indistinguishable from the uninjected side (Figs. 3E-G). Comparable expression of Gag at the different levels along the rostralcaudal axis (Figs. 3G, 3J, 3M) indicated that the lack of abnormalities in cartilage differentiation in the caudal region is related to a more advanced stage of differentiation of cartilage at the time of peak infection. In the

middle region, the decrease in the domain of *aggrecan* expression (Fig. 3H) was more noticeable than *Sox9* (Fig. 3I) indicating the negative effects of dnFGFR3 on differentiation of *Sox9*-expressing cells. Rostral/growing ends of Meckel's cartilage on the injected side showed decreases in the intensity and domain of *Sox9* expression and a lack of *aggrecan* expression (Figs. 3K-M) showing the negative effects of dnFGFR3 on differentiation of *Sox9*-expressing cells in the growing end, leading to the formation of truncated/shortened Meckel's cartilage (Fig. 1B). Analysis of cell proliferation and apoptosis showed a 50% decrease in the number of proliferative cells and a greater than four fold increase in the number of apoptotic cells in the newly formed Meckel's cartilage in the injected sides (Table 2, Fig. 4B), revealing the roles of FGF/FGFR3 on proliferation and survival of the chondroblasts in Meckel's cartilage.

The roles of FGF/FGFR3 on the proliferation of chondroblasts and the elongation of Meckel's cartilage were further supported by decreases in the number of proliferative chondroblasts in the rostral/growing end of the Meckel's cartilage on the injected side four days after injection. The rostral region of Meckel's cartilage on the uninjected side contained a significantly greater number (55%) of proliferative chondroblasts compared to the middle and caudal regions (Table 2). In contrast, the number of proliferative chondroblasts in the rostral end of the Meckel's cartilage on the injected side was comparable to those in the middle and caudal regions and decreased as compared to the uninjected side (Table 2). Apoptotic cells were not detected in Meckel's cartilage in either the injected or uninjected sides (Table 2). However, there was a greater than three fold increase in the number of apoptotic cells in the mesenchyme rostral to the growing end of Meckel's cartilage on the injected sides (196.6 ± 10.9) compared to the uninjected side (58.9 ± 13.3).

Together these observations show roles for FGF/FGFR3 signaling in proliferation, survival and overt differentiation of *Sox9*-expressing chondro-progenitors and chondroblasts in Meckel's cartilage.

dnFGFR3 affected *in vitro* chondrogenesis

The role of FGF/FGFR3 signaling in chondrogenesis by the mandibular mesenchyme was further examined in high-density micromass cultures derived from HH23 mandibular mesenchyme. This culture system allows the formation of chondrogenic condensations and differentiation, and is a useful tool for examining the roles of signaling pathways during various stages of chondrogenesis.

Immunohistochemical analysis showed Gag and dnFGFR3 positive cells within cartilaginous nodules and in the inter-nodular regions (Supplemental Figs. 3E, 3F). Infection with RCAS-dnFGFR3 resulted in reduced chondrogenesis as demonstrated by significant decreases in the area and the amount of Alcian blue-stained matrix (Figs. 4G, 4H and Table 3). The decreases in chondrogenic differentiation were not related to decreases in the size of cultures, as the total area of micromass cultures was comparable among cultures infected with control virus and RCAS-dnFGFR3 (Figs. 4G and 4H). Infection with control virus did not affect chondrogenesis of mandibular mesenchyme as compared to uninfected cultures (data not shown). The reduced chondrogenesis in high density cultures derived from mandibular mesenchyme infected with dnFGFR3 is consistent with impaired chondrogenesis in micromass cultures from *Fgfr3*−/− limb buds (Davidson et al., 2005).

The effects of dnFGFR3 on chondrogenic condensation *in vitro* was examined by staining with PNA, a lectin that selectively binds a cell surface marker(s) on condensing mesenchyme (Zimmermann and Thies, 1984). Cultures infected with RCAS-dnFGFR3 showed decreases in the number, but not the size of PNA-positive chondrogenic condensations compared to cultures infected with control RCAS (Table 3). Morphometric analysis of cartilage nodules in

cultures stained with both PNA and Alcian blue showed increases in the ratio of PNA to Alcian blue staining in cultures infected with dnFGFR3 compared to control virus (Table 3), showing the negative effects of dnFGFR3 on differentiation of the PNA-positive cells at the periphery of the micromass cultures. In cultures infected with control virus, nearly the entire area of the cartilage nodules stained with Alcian blue, whereas in cultures infected with RCAS-dnFGFR3, Alcian blue-stained cartilage nodules were surrounded by PNA-positive cells on the periphery (not shown).

dnFGFR3 affects osteogenic condensations and appositional growth of mandibular bones

Skeletal staining at HH37 showed that all embryos injected with RCAS-dnFGFR3 displayed abnormalities in five of the mandibular bones on the injected sides (Table 1 and Figs. 1B, C, D). Injections at early stages led to absence of bones (articular, angular, supra-angular, dentary and splenial, Table 1 and Fig. 1B) whereas injection at HH26 led to the formation of smaller bones in the caudal region (articular, angular, supra-angular) and absence of the bones in the rostral region (dentary and splenial bones, Table 1 and Figs. 1C, 1D). These abnormalities are consistent with the patterns of expression of *Fgfr3* in the developing mandibular bones. *Fgfr3* is initially expressed in osteogenic condensations and later in the osteoblasts and periosteal tissues expressing *PTH-1R* (Supplemental Fig. 1).

The difference in the effects of RCAS-dnFGFR3 in the caudal vs. more rostral bones after injection at later stages is related to the stage of differentiation of different mandibular bones along the caudal-rostral axis of the mandible at the time of peak infection (Mina et al., 2007). The lack of abnormalities in the mento-mandibular bone after injection of dnFGFR3 at all stages (Figs. 1B-D, Table 1) suggest that development of the mento-mandibular bone is not dependent on FGF/FGFR3 signaling and is dependent on other signaling pathways, such as the ET-1-dHAND-Msx1 and BMP/Alk2 signaling pathways shown to play critical roles in the morphogenesis of the medial/rostral region of the mandible (Dudas et al., 2004; Fukuhara et al., 2004; Thomas et al., 1998).

To exclude the possibility that the abnormalities in the mandibular bones were related to severe defects in the outgrowth of the mandibular process and Meckel's cartilage, RCAS-dnFGFR3 was injected into the right maxillary process at early stages (n=8). This treatment did not affect the outgrowth of the maxillary process but led to the absence of bones derived from the maxillary process (maxillary bone, palatal process and jugal bone, Figs. 1E, F).

Next we examined the patterns of expression of early (*PTH-1R* and *Runx2*) and late (*Osteocalcin, OC*) markers of osteoblast differentiation, as well as changes in apoptosis and proliferation in angular and supra-angular bones, as these bones were easily identifiable in cross sections and were consistently affected after both early and late injections (Table 1).

Four days after injection at early stages, the region corresponding to the osteogenic condensations giving rise to the supra-angular and angular bones on the injected side showed a lack of expression of both *PTH-1R* and *Runx2* (Fig. 5B and data not shown), a 51% decrease in the number of proliferative cells, and an approximately 78% increase in the number of apoptotic cells (Table 2). These changes, together with the lack of histological evidence for osteogenic condensation in Hematoxylin and Eosin stained sections (Fig. 5A) revealed the essential roles of FGF/FGFR3 on proliferation and survival of osteo-progenitor cells in osteogenic condensations.

Analyses of the angular bone six days after late injection at HH26 showed significant reductions in the domains of expression of *PTH-1R, Runx2* and *OC,* a 24% decrease in the number of proliferating cells, and a 70% increase in apoptosis compared to the uninjected side (Table 2 and Figs. 5C-K). Osteoblasts on the injected side expressed *PTH-1R* and *OC,* but low or no

detectable *Runx2* (Figs. 5C-K). These results showed that FGF/FGFR3 is essential for proliferation and survival of osteoblasts and the osteoprogenitors in the periosteum.

Effects of dominant negative FGFR2 on the formation of Meckel's cartilage and mandibular osteogenesis

The patterns of expression of *Fgfr2* in the developing chick mandibular skeleton are similar to *Fgfr3* (Supplemental Fig. 1), suggesting the possibility of redundant and/or cooperative roles for FGFR2c and FGFR3c in the chondrogenesis and osteogenesis of the mandibular mesenchyme. The role of FGFR2c-mediated signaling in the formation and elongation of Meckel's cartilage and mandibular osteogenesis was examined using a previously characterized RCAS-dnFGFR2 shown to decrease proliferation in primary osteoblast cultures (Ratisoontorn et al., 2003).

Skeletal staining after early injection of RCAS-dnFGFR2 (n=32) revealed the formation of slightly smaller articular, angular, supra-angular, and splenial bones on the injected side of 90% of the embryos (Fig. 1G, Table 1). The formation of smaller mandibular bones on the injected sides in our study is consistent with roles of FGF/FGFR2c in osteoblast proliferation and differentiation (Eswarakumar et al., 2002;Yu et al., 2003). Mice lacking the *Fgfr2c* isoform (Eswarakumar et al., 2002) and conditional inactivation of *Fgfr2* in the osteogenic lineage (Yu et al., 2003) showed delayed onset of osteoblast differentiation with decreases in *Runx2* expression (Eswarakumar et al., 2002).

However, there were no severe abnormalities in the outgrowth of the mandibular processes or morphogenesis of Meckel's cartilage on the injected side (Fig. 1G). Furthermore, RCAS-dnFGFR2 had no discernable effect on *in vitro* chondrogenesis of mandibular mesenchyme (Table 3). The lack of noticeable abnormalities on *in vivo* and *in vitro* chondrogenesis of mandibular mesenchyme by dnFGFR2 was not related to unsuccessful infection or inability of dnFGFR2 to act as a dominant negative receptor. Western blot analysis of DF-1 cells infected with RCAS-dnFGFR2 showed the presence of an intact protein product of approximately 82kDa (Supplemental Fig. 2B). Immunohistochemical analysis showed widespread expression of Gag and HA-tagged dnFGFR2 in the injected side of mandibles and in infected micromass cultures (Supplemental Figs. 3D, G, H, and data not shown). RCAS-dnFGFR2 also resulted in a markedly reduced mitogenic response to FGF2 (Supplemental Fig. 2C). Furthermore, injection of RCAS-dnFGFR2 in the developing forelimb at HH19−20 (n=7) led to shortening of the entire limb and various skeletal elements (Fig. 1H). Skeletal preparations at HH37 showed shortened ossified regions in the humerus (4/7), radius (5/7) and ulna (3/7) in the injected limbs. Other abnormalities included a lack of osteogenesis in the proximal phalanges and truncations of the cartilaginous middle and distal phalanges (7/7) (Fig. 1H). These changes in the developing limb are consistent with the abnormalities in mice lacking FGFR2c (Eswarakumar et al., 2002;Yu et al., 2003).

Discussion

Our expression data together with our analysis of the effects of blocking FGFR3 and FGFR2 signaling on mandibular skeletogenesis provide new evidence for essential roles of FGF/FGFR3 signaling in the formation of osteogenic condensations, and in the morphogenesis and elongation of Meckel's cartilage. Our study also shows that appositional growth of mandibular bones is dependent on both FGFR2 and FGFR3 signaling.

Roles for FGF signaling during morphogenesis and elongation of Meckel's cartilage

Our observations show that blocking FGFR3 signaling in the developing chick mandible between HH17−20 did not affect the initial formation of Meckel's cartilage but affected further

morphogenesis and the elongation of Meckel's cartilage. Blocking FGFR3 signaling affected the proliferation, survival and differentiation of cells within the chondrogenic mesenchyme and chondroblasts. This provides new evidence for the essential roles of FGF/FGFR3 signaling during the morphogenesis and elongation of Meckel's cartilage.

We have shown that blocking FGFR3 signaling during the formation of Meckel's cartilage led to the truncation of the rostral/growing end of the Meckel's cartilage. The effects were mediated by decreased proliferation of chondroblasts in Meckel's cartilage and impaired differentiation of *Sox9* expressing chondrogenic cells. The essential role of FGFR3 signaling on proliferation of chondrogenic cells in Meckel's cartilage in chick embryos provides support for mitogenic effects of FGFR3 signaling on chondroblasts/chondrocytes during embryonic development. The positive roles of FGFR3 mediated signaling on chondrocyte proliferation and differentiation are different from the negative roles of FGFR3 on chondrocytes during the postnatal stages of development (Colvin et al., 1996; Deng et al., 1996; Eswarakumar and Schlessinger, 2007). Although a comprehensive analysis of craniofacial defects in *Fgfr3*−/− and *Fgfr3c*−/− mice during embryonic development has not been reported, a lack of defects in the developing mandible and Meckel's cartilage in these transgenic mice may not be surprising as the main body of the Meckel's cartilage in mammals is a transient structure (Harada and Ishizeki, 1998). The permanent fate of Meckel's cartilage in birds as compared to its transient fate in mammals allowed us to gain insight into roles of FGF/FGFR3 in morphogenesis of Meckel's cartilage. The positive roles of FGFR3 signaling on proliferation of chondroblasts during early embryonic development in our study are also supported by findings in transgenic mice carrying an activating mutation in FGFR3 (Iwata et al., 2000; Iwata et al., 2001). These animals displayed increases in the proliferation of chondroblasts in the growth plate at E15.5 (Iwata et al., 2000; Iwata et al., 2001) and overgrowth of other hyaline cartilages, including the trachea and nasal septum (Iwata et al., 2001).

Our observations also show essential roles of FGF/FGFR3 signaling in the survival and differentiation of *Sox9*-expressing chondrogenic cells. *Sox9* is a transcription factor that is expressed in chondrogenic mesenchyme with critical roles in the overt differentiation of chondrocytes and their survival and proliferation (Lefebvre et al., 1998). Inactivation of *Sox9* in limb buds prior to the formation of chondrogenic condensations led to an absence of cartilage elements (Akiyama et al., 2002). Inactivation of *Sox9* in condensed mesenchymal cells and differentiated chondrocytes revealed the essential roles of *Sox9* in proliferation, survival and overt differentiation of chondroblasts (Akiyama et al., 2002). The truncation of Meckel's cartilage and the hypoplastic mandibular processes on the injected side in our study suggest that the effects of FGFR3 signaling on Meckel's cartilage are mediated at least in part through *Sox9*. This is further supported by the similarities in the changes observed in our study and those reported in *Sox9*−/+ mutant mice (Bi et al., 2001),

The overlapping expression patterns of FGFR2c and FGFR3c in the chondrogenic condensation and the newly formed Meckel's cartilage suggest the possibility of cooperative/redundant roles of these receptors in the morphogenesis of Meckel's cartilage. However, our study shows that despite wide expression, dnFGFR2 did not affect chondrogenesis and elongation of Meckel's cartilage *in vivo* or *in vitro*, suggesting dispensable/unessential roles of FGFR2 signaling in this process. Since the peak expression of dnFGFR2 and dnFGFR3 occurs during the formation of the chondrogenic condensation, the roles of signaling through these receptors during early stages of mandibular morphogenesis remains unknown.

Roles for FGF signaling during osteogenesis of the mandibular bones

The importance of FGFRs in osteogenesis has been highlighted by the discoveries that gain-of-function point mutations within the amino acid coding sequences of FGFRs1−3 are responsible for craniosynostoses syndromes, characterized by premature fusion of cranial

sutures due to dysregulated intramembranous bone formation (Ornitz and Marie, 2002). FGFR1 stimulates osteoblast differentiation (Hajihosseini et al., 2004; Iseki et al., 1999; Zhou et al., 2000). FGFR2 is involved in regulating osteoblast proliferation and differentiation (reviewed by Eswarakumar et al., 2005; Ornitz and Marie, 2002). The formation of mandibular bones with reduced size after injection of dnFGFR2 is consistent with essential roles of FGF/FGFR2 signaling in osteoblast proliferation and differentiation.

Moreover, our results provide new evidence for the essential roles FGF/FGFR3 signaling in the survival, proliferation and differentiation of osteoprogenitors within the osteogenic condensations and periosteum of the chick mandibular bones. We show that blocking FGFR3 signaling at early stages of mandibular development resulted in decreased cell survival and proliferation and a complete absence of osteogenic mesenchyme. We also show that blocking FGFR3 signaling at later stages of mandibular development after the formation of osteogenic mesenchyme resulted in smaller bones through its effects on survival and proliferation of osteoblasts and osteoprogenitor cells within the periosteum, which is responsible for appositional growth of the mandibular bones.

The roles of FGFR3 signaling in mandibular osteogenesis support the recent observations in several transgenic mouse models (Ornitz, 2005; Ornitz and Marie, 2002). Transgenic mice carrying an activating (G375C) mutation in FGFR3 displayed increased expression of markers of osteoblast differentiation and advanced ossification in the long bones (Chen et al., 1999). Inhibition of FGFR3 expression by Twist inhibited the differentiation of osteoprogenitor cells into osteoblasts (Funato et al., 2001). More recently it has been shown that young adult *Fgfr3* −/− and *Fgfr3c*−/− mice were osteopenic and displayed decreased thickness of cortical and trabecular bones (Valverde-Franco et al., 2004, Eswarakumar and Schlessinger, 2007). In the long bones, cortical bone in the diaphyses is formed by direct differentiation of osteoprogenitor cells in the periosteum into osteoblasts, a process that is similar to intramembranous ossification, providing additional support for essential roles for FGF/FGFR3 signaling in intramembranous ossification. Interestingly, FGFR3 is detected in sutural osteogenic fronts (Rice et al., 2000; Rice et al., 2003), and Saethre-Chotzen syndrome associated craniosynostosis is caused by mutations in the gene encoding *TWIST* or *FGFR3* (Chun et al., 2002).

The change in the expression of *Runx2* in our study suggests that the effects of FGF signaling in osteoblasts are mediated through *Runx2*. *Runx2* is expressed in osteogenic condensations and acts as an osteoblast differentiation factor (reviewed by Stein et al., 2004). Runx2 is also expressed in terminally differentiated osteoblasts, where it directly stimulates transcription of osteoblast-related genes (reviewed by Franceschi and Xiao, 2003; Stein et al., 2004). Runx2 expression and functional activity are controlled by the mitogen-activated protein kinase (MAPK) pathway activated by a variety of signals, including those initiated by FGFs (Franceschi and Xiao, 2003).

However, it is possible that the effects of dnFGFR3 on mandibular osteogenesis may be indirect and mediated by regulating angiogenesis. *Fgfr3*−/− mice showed a down-regulation of vascular endothelial growth factor (VEGF) (Amizuka et al., 2004), whereas transgenic mice carrying an activating mutation in FGFR3 (G380R) displayed premature and increased vascularization (Cormier et al., 2002; Segev et al., 2000).

Potential FGF ligands involved in mandibular skeletogenesis

Our observations reveal essential roles of FGFs capable of binding with high affinity to FGFR3 in the morphogenesis of avian Meckel's cartilage and mandibular bones. Binding studies have shown that FGFR3b and FGFR3c isoforms are both activated by FGF1 and by FGF9 (Ornitz

et al., 1996; Zhang et al., 2006). In addition, FGFs 2, 4, 6, 8 and 18 also bind with high affinity to FGFR3c (Ornitz et al., 1996; Zhang et al., 2006).

A growing body of evidence indicates that among these ligands, FGF18 is the most likely physiological ligand for FGFR3 in both osteogenesis and chondrogenesis (Davidson et al., 2005; Ellsworth et al., 2002; Liu et al., 2007; Liu et al., 2002; Ohbayashi et al., 2002; Reinhold et al., 2004). *In vitro* studies have shown that FGF18 can bind to and interact strongly with FGFR3c, moderately with FGFR2c, but not with FGFR1c (Zhang et al., 2006). Analysis of abnormalities in mice lacking *Fgf18* at different developmental stages has provided evidence for both positive and negative roles of FGF18/FGFR3 signaling on chondrocyte proliferation during early and later stages of development respectively (Liu et al., 2007; Liu et al., 2002; Ohbayashi et al., 2002). The hypoplastic mandible and shortened Meckel's cartilage in *Fgf18* −/− mice (Liu et al., 2007), together with expression of *Fgf18* in the chondrogenic mesenchyme and perichondrium of Meckel's cartilage in human fetuses (Cormier et al., 2005), provide support for roles of FGF18/FGFR3 signaling in the morphogenesis and elongation of Meckel's cartilage.

Fgf18−/− mice also displayed delayed ossification in the skeletal elements formed by both endochondral and intramembranous ossification (Liu et al., 2007; Liu et al., 2002; Ohbayashi et al., 2002). Young adult $Fgf18^{-/-}$ mice, similar to *Fgfr3*−/− mice (Amizuka et al., 2004), were dwarfed, showed decreased expression of VEGF, *Runx2*, *osteopontin*, and *osteocalcin* suggesting that the roles of FGF18/FGFR3 in osteogenesis, including intramembranous ossification of chick mandible in our study, are indirect.

Specificity of dnFGFR Approach

In a complex system such as the developing mandible with overlapping patterns of expression of *Fgfrs*, one possible explanation of our findings is that the abnormalities caused by dnFGFR3 are the result of a general dominant-negative effect by sequestering various FGFs and/or by inhibition of signaling through other FGFRs. This possibility is difficult to reconcile with our data as dnFGFR2 led to a markedly milder phenotype, and there were no changes in the morphogenesis of the tongue and mandibular muscles, shown to be dependent on signaling through FGFR1 and FGFR4 (Flanagan-Steet et al., 2000; Marics et al., 2002). The milder phenotype caused by dnFGFR2 may be caused by heterodimerization of dnFGFR2 with FGFR3c.

Acknowledgements

We thank all the individuals providing reagents, Dr. Kullen Gallagher for his assistance in the expression of *Fgfrs* in the mandible, Ms. Barbara Rodgers for technical assistance in all aspects of this work, and Dr. William Upholt for critical reading of the manuscript. This work was supported by NIH grant R01 DE08682 to MM. Bruce Havens is grateful for the support of the Institutional Dental Scientist Award (NICDR grant K16 DE00157).

References

Abu-Issa R, Smyth G, Smoak I, Yamamura K, Meyers EN. Fgf8 is required for pharyngeal arch and cardiovascular development in the mouse. Development 2002;129:4613–25. [PubMed: 12223417]

Akiyama H, Chaboissier MC, Martin JF, Schedl A, de Crombrugghe B. The transcription factor Sox9 has essential roles in successive steps of the chondrocyte differentiation pathway and is required for expression of Sox5 and Sox6. Genes Dev 2002;16:2813–28. [PubMed: 12414734]

Amizuka N, Davidson D, Liu H, Valverde-Franco G, Chai S, Maeda T, Ozawa H, Hammond V, Ornitz DM, Goltzman D, Henderson JE. Signalling by fibroblast growth factor receptor 3 and parathyroid hormone-related peptide coordinate cartilage and bone development. Bone 2004;34:13–25. [PubMed: 14751559]

Barlow AJ, Bogardi JP, Ladher R, Francis-West PH. Expression of chick Barx-1 and its differential regulation by FGF-8 and BMP signaling in the maxillary primordia. Dev Dyn 1999;214:291–302. [PubMed: 10213385]

Bi W, Huang W, Whitworth DJ, Deng JM, Zhang Z, Behringer RR, de Crombrugghe B. Haploinsufficiency of Sox9 results in defective cartilage primordia and premature skeletal mineralization. Proc Natl Acad Sci U S A 2001;98:6698–703. [PubMed: 11371614]

Bobick BE, Kulyk WM. MEK-ERK signaling plays diverse roles in the regulation of facial chondrogenesis. Exp Cell Res 2006;312:1079–92. [PubMed: 16457813]

Bobick BE, Thornhill TM, Kulyk WM. Fibroblast growth factors 2, 4, and 8 exert both negative and positive effects on limb, frontonasal, and mandibular chondrogenesis via MEK-ERK activation. J Cell Physiol 2007;211:233–43. [PubMed: 17167778]

Chai Y, Maxson RE Jr. Recent advances in craniofacial morphogenesis. Dev Dyn 2006;235:2353–75. [PubMed: 16680722]

Chen L, Adar R, Yang X, Monsonego EO, Li C, Hauschka PV, Yayon A, Deng CX. Gly369Cys mutation in mouse FGFR3 causes achondroplasia by affecting both chondrogenesis and osteogenesis. J Clin Invest 1999;104:1517–25. [PubMed: 10587515]

Chun K, Teebi AS, Jung JH, Kennedy S, Laframboise R, Meschino WS, Nakabayashi K, Scherer SW, Ray PN, Teshima I. Genetic analysis of patients with the Saethre-Chotzen phenotype. Am J Med Genet 2002;110:136–43. [PubMed: 12116251]

Colvin JS, Bohne BA, Harding GW, McEwen DG, Ornitz DM. Skeletal overgrowth and deafness in mice lacking fibroblast growth factor receptor 3. Nat Genet 1996;12:390–7. [PubMed: 8630492]

Cormier S, Delezoide AL, Benoist-Lasselin C, Legeai-Mallet L, Bonaventure J, Silve C. Parathyroid hormone receptor type 1/Indian hedgehog expression is preserved in the growth plate of human fetuses affected with fibroblast growth factor receptor type 3 activating mutations. Am J Pathol 2002;161:1325–35. [PubMed: 12368206]

Cormier S, Leroy C, Delezoide AL, Silve C. Expression of fibroblast growth factors 18 and 23 during human embryonic and fetal development. Gene Expr Patterns 2005;5:569–73. [PubMed: 15749088]

Crump JG, Maves L, Lawson ND, Weinstein BM, Kimmel CB. An essential role for Fgfs in endodermal pouch formation influences later craniofacial skeletal patterning. Development 2004a;131:5703–16. [PubMed: 15509770]

Crump JG, Swartz ME, Kimmel CB. An integrin-dependent role of pouch endoderm in hyoid cartilage development. Plos Biology 2004b;2:E244. [PubMed: 15269787]

David NB, Saint-Etienne L, Tsang M, Schilling TF, Rosa FM. Requirement for endoderm and FGF3 in ventral head skeleton formation. Development 2002;129:4457–68. [PubMed: 12223404]

Davidson D, Blanc A, Filion D, Wang H, Plut P, Pfeffer G, Buschmann MD, Henderson JE. Fibroblast growth factor (FGF) 18 signals through FGF receptor 3 to promote chondrogenesis. J Biol Chem 2005;280:20509–15. [PubMed: 15781473]

Deng C, Wynshaw-Boris A, Zhou F, Kuo A, Leder P. Fibroblast growth factor receptor 3 is a negative regulator of bone growth. Cell 1996;84:911–21. [PubMed: 8601314]

Dudas M, Sridurongrit S, Nagy A, Okazaki K, Kaartinen V. Craniofacial defects in mice lacking BMP type I receptor Alk2 in neural crest cells. Mech Dev 2004;121:173–82. [PubMed: 15037318]

Ellsworth JL, Berry J, Bukowski T, Claus J, Feldhaus A, Holderman S, Holdren MS, Lum KD, Moore EE, Raymond F, Ren H, Shea P, Sprecher C, Storey H, Thompson DL, Waggie K, Yao L, Fernandes RJ, Eyre DR, Hughes SD. Fibroblast growth factor-18 is a trophic factor for mature chondrocytes and their progenitors. Osteoarthritis Cartilage 2002;10:308–20. [PubMed: 11950254]

Erceg I, Tadic T, Kronenberg MS, Marijanovic I, Lichtler AC. Dlx5 regulation of mouse osteoblast differentiation mediated by avian retrovirus vector. Croat Med J 2003;44:407–11. [PubMed: 12950142]

Eswarakumar VP, Lax I, Schlessinger J. Cellular signaling by fibroblast growth factor receptors. Cytokine Growth Factor Rev 2005;16:139–49. [PubMed: 15863030]

Eswarakumar VP, Monsonego-Ornan E, Pines M, Antonopoulou I, Morriss-Kay GM, Lonai P. The IIIc alternative of Fgfr2 is a positive regulator of bone formation. Development 2002;129:3783–93. [PubMed: 12135917]

Eswarakumar VP, Schlessinger J. Skeletal overgrowth is mediated by deficiency in a specific isoform of fibroblast growth factor receptor 3. Proc Natl Acad Sci U S A 2007;104:3937–42. [PubMed: 17360456]

Ferrari D, Harrington A, Dealy CN, Kosher RA. Dlx-5 in limb initiation in the chick embryo. Dev Dyn 1999;216:10–5. [PubMed: 10474161]

Flanagan-Steet H, Hannon K, McAvoy MJ, Hullinger R, Olwin BB. Loss of FGF receptor 1 signaling reduces skeletal muscle mass and disrupts myofiber organization in the developing limb. Dev Biol 2000;218:21–37. [PubMed: 10644408]

Franceschi RT, Xiao G. Regulation of the osteoblast-specific transcription factor, Runx2: responsiveness to multiple signal transduction pathways. J Cell Biochem 2003;88:446–54. [PubMed: 12532321]

Francis-West PH, Robson L, Evans DJ. Craniofacial development: the tissue and molecular interactions that control development of the head. Adv Anat Embryol Cell Biol 2003;169:III–VI. 1–138. [PubMed: 12793205]

Frank DU, Fotheringham LK, Brewer JA, Muglia LJ, Tristani-Firouzi M, Capecchi MR, Moon AM. An Fgf8 mouse mutant phenocopies human 22q11 deletion syndrome. Development 2002;129:4591–603. [PubMed: 12223415]

Fukuhara S, Kurihara Y, Arima Y, Yamada N, Kurihara H. Temporal requirement of signaling cascade involving endothelin-1/endothelin receptor type A in branchial arch development. Mech Dev 2004;121:1223–33. [PubMed: 15327783]

Funato N, Ohtani K, Ohyama K, Kuroda T, Nakamura M. Common regulation of growth arrest and differentiation of osteoblasts by helix-loop-helix factors. Mol Cell Biol 2001;21:7416–28. [PubMed: 11585922]

Gehris AL, Stringa E, Spina J, Desmond ME, Tuan RS, Bennett VD. The region encoded by the alternatively spliced exon IIIA in mesenchymal fibronectin appears essential for chondrogenesis at the level of cellular condensation. Dev Biol 1997;190:191–205. [PubMed: 9344538]

Hajihosseini MK, Lalioti MD, Arthaud S, Burgar HR, Brown JM, Twigg SR, Wilkie AO, Heath JK. Skeletal development is regulated by fibroblast growth factor receptor 1 signalling dynamics. Development 2004;131:325–35. [PubMed: 14668415]

Hamburger V, Hamilton HL. A series of normal stages in the development of the chick embryo. J Morph 1951;88:49–92.

Harada Y, Ishizeki K. Evidence for transformation of chondrocytes and site-specific resorption during the degradation of Meckel's cartilage. Anat Embryol (Berl) 1998;197:439–50. [PubMed: 9682975]

Hassell JR, Horigan EA. Chondrogenesis: a model developmental system for measuring teratogenic potential of compounds. Teratog Carcinog Mutagen 1982;2:325–31. [PubMed: 6130632]

Havens BA, Rodgers B, Mina M. Tissue-specific expression of Fgfr2b and Fgfr2c isoforms, Fgf10 and Fgf9 in the developing chick mandible. Arch Oral Biol 2006;51:134–45. [PubMed: 16105644]

Healy C, Uwanogho D, Sharpe PT. Regulation and role of Sox9 in cartilage formation. Dev Dyn 1999;215:69–78. [PubMed: 10340758]

Hendzel MJ, Wei Y, Mancini MA, Van Hooser A, Ranalli T, Brinkley BR, Bazett-Jones DP, Allis CD. Mitosis-specific phosphorylation of histone H3 initiates primarily within pericentromeric heterochromatin during G2 and spreads in an ordered fashion coincident with mitotic chromosome condensation. Chromosoma 1997;106:348–60. [PubMed: 9362543]

Iseki S, Wilkie AO, Morriss-Kay GM. Fgfr1 and Fgfr2 have distinct differentiation- and proliferation-related roles in the developing mouse skull vault. Development 1999;126:5611–20. [PubMed: 10572038]

Iwata T, Chen L, Li C, Ovchinnikov DA, Behringer RR, Francomano CA, Deng CX. A neonatal lethal mutation in FGFR3 uncouples proliferation and differentiation of growth plate chondrocytes in embryos. Hum Mol Genet 2000;9:1603–13. [PubMed: 10861287]

Iwata T, Li CL, Deng CX, Francomano CA. Highly activated Fgfr3 with the K644M mutation causes prolonged survival in severe dwarf mice. Hum Mol Genet 2001;10:1255–64. [PubMed: 11406607]

Le Douarin NM, Creuzet S, Couly G, Dupin E. Neural crest cell plasticity and its limits. Development 2004;131:4637–50. [PubMed: 15358668]

Lefebvre V, Li P, de Crombrugghe B. A new long form of Sox5 (L-Sox5), Sox6 and Sox9 are coexpressed in chondrogenesis and cooperatively activate the type II collagen gene. Embo J 1998;17:5718–33. [PubMed: 9755172]

Liu Z, Lavine KJ, Hung IH, Ornitz DM. FGF18 is required for early chondrocyte proliferation, hypertrophy and vascular invasion of the growth plate. Dev Biol 2007;302:80–91. [PubMed: 17014841]

Liu Z, Xu J, Colvin JS, Ornitz DM. Coordination of chondrogenesis and osteogenesis by fibroblast growth factor 18. Genes Dev 2002;16:859–69. [PubMed: 11937493]

Lizarraga G, Lichtler A, Upholt WB, Kosher RA. Studies on the role of Cux1 in regulation of the onset of joint formation in the developing limb. Dev Biol 2002;243:44–54. [PubMed: 11846476]

Macatee TL, Hammond BP, Arenkiel BR, Francis L, Frank DU, Moon AM. Ablation of specific expression domains reveals discrete functions of ectoderm- and endoderm-derived FGF8 during cardiovascular and pharyngeal development. Development 2003;130:6361–74. [PubMed: 14623825]

Marics I, Padilla F, Guillemot JF, Scaal M, Marcelle C. FGFR4 signaling is a necessary step in limb muscle differentiation. Development 2002;129:4559–69. [PubMed: 12223412]

Meyer MP, Swann K, Burnstock G, Clarke JD. The extracellular ATP receptor, cP2Y(1), inhibits cartilage formation in micromass cultures of chick limb mesenchyme. Dev Dyn 2001;222:494–505. [PubMed: 11747083]

Mina M. Regulation of mandibular growth and morphogenesis. Crit Rev Oral Biol Med 2001;12:276–300. [PubMed: 11603502]

Mina M, Gluhak J, Upholt WB, Kollar EJ, Rogers B. Experimental analysis of Msx-1 and Msx-2 gene expression during chick mandibular morphogenesis. Dev Dyn 1995;202:195–214. [PubMed: 7734736]

Mina M, Havens B, Velonis DA. FGF signaling in mandibular skeletogenesis. Orthod Craniofac Res 2007;10:59–66. [PubMed: 17552942]

Mina M, Upholt WB, Kollar EJ. Stage-related chondrogenic potential of avian mandibular ectomesenchymal cells. Differentiation 1991;48:9–16. [PubMed: 1743432]

Mina M, Wang YH, Ivanisevic AM, Upholt WB, Rodgers B. Region- and stage-specific effects of FGFs and BMPs in chick mandibular morphogenesis. Dev Dyn 2002;223:333–52. [PubMed: 11891984]

Miyake T, Cameron AM, Hall BK. Stage-specific onset of condensation and matrix deposition for Meckel's and other first arch cartilages in inbred C57BL/6 mice. J Craniofac Genet Dev Biol 1996;16:32–47. [PubMed: 8675613]

Morgan BA, Fekete DM. Manipulating gene expression with replication-competent retroviruses. Methods Cell Biol 1996;51:185–218. [PubMed: 8722477]

Neugebauer BM, Moore MA, Broess M, Gerstenfeld LC, Hauschka PV. Characterization of structural sequences in the chicken osteocalcin gene: expression of osteocalcin by maturing osteoblasts and by hypertrophic chondrocytes in vitro. J Bone Miner Res 1995;10:157–63. [PubMed: 7747623]

Nie X, Luukko K, Kettunen P. FGF signalling in craniofacial development and developmental disorders. Oral Dis 2006;12:102–11. [PubMed: 16476029]

Nissen RM, Yan J, Amsterdam A, Hopkins N, Burgess SM. Zebrafish foxi one modulates cellular responses to Fgf signaling required for the integrity of ear and jaw patterning. Development 2003;130:2543–54. [PubMed: 12702667]

Ohbayashi N, Shibayama M, Kurotaki Y, Imanishi M, Fujimori T, Itoh N, Takada S. FGF18 is required for normal cell proliferation and differentiation during osteogenesis and chondrogenesis. Genes Dev 2002;16:870–9. [PubMed: 11937494]

Oliver BL, Sha'afi RI, Hajjar JJ. Transforming growth factor-alpha increases tyrosine phosphorylation of microtubule-associated protein kinase in a small intestinal crypt cell line (IEC-6). Biochem J 1994;303(Pt 2):455–60. [PubMed: 7980404]

Ornitz DM. FGF signaling in the developing endochondral skeleton. Cytokine Growth Factor Rev 2005;16:205–13. [PubMed: 15863035]

Ornitz DM, Marie PJ. FGF signaling pathways in endochondral and intramembranous bone development and human genetic disease. Genes Dev 2002;16:1446–65. [PubMed: 12080084]

Ornitz DM, Xu J, Colvin JS, McEwen DG, MacArthur CA, Coulier F, Gao G, Goldfarb M. Receptor specificity of the fibroblast growth factor family. J Biol Chem 1996;271:15292–7. [PubMed: 8663044]

Potts WM, Olsen M, Boettiger D, Vogt VM. Epitope mapping of monoclonal antibodies to gag protein p19 of avian sarcoma and leukaemia viruses. J Gen Virol 1987;68(Pt 12):3177–82. [PubMed: 2447226]

Ratisoontorn C, Fan GF, McEntee K, Nah HD. Activating (P253R, C278F) and dominant negative mutations of FGFR2: differential effects on calvarial bone cell proliferation, differentiation, and mineralization. Connect Tissue Res 2003;44(Suppl 1):292–7. [PubMed: 12952211]

Reinhold MI, Abe M, Kapadia RM, Liao Z, Naski MC. FGF18 represses noggin expression and is induced by calcineurin. J Biol Chem 2004;279:38209–19. [PubMed: 15252029]

Rice DP, Aberg T, Chan Y, Tang Z, Kettunen PJ, Pakarinen L, Maxson RE, Thesleff I. Integration of FGF and TWIST in calvarial bone and suture development. Development 2000;127:1845–55. [PubMed: 10751173]

Rice DP, Rice R, Thesleff I. Fgfr mRNA isoforms in craniofacial bone development. Bone 2003;33:14–27. [PubMed: 12919696]

Richman JM, Herbert M, Matovinovic E, Walin J. Effect of fibroblast growth factors on outgrowth of facial mesenchyme. Dev Biol 1997;189:135–47. [PubMed: 9281343]

Richman JM, Lee SH. About face: signals and genes controlling jaw patterning and identity in vertebrates. Bioessays 2003;25:554–68. [PubMed: 12766945]

Santagati F, Rijli FM. Cranial neural crest and the building of the vertebrate head. Nat Rev Neurosci 2003;4:806–18. [PubMed: 14523380]

Schneider RA, Helms JA. The cellular and molecular origins of beak morphology. Science 2003;299:565–8. [PubMed: 12543976][see comment]

Segev O, Chumakov I, Nevo Z, Givol D, Madar-Shapiro L, Sheinin Y, Weinreb M, Yayon A. Restrained chondrocyte proliferation and maturation with abnormal growth plate vascularization and ossification in human FGFR-3(G380R) transgenic mice. Hum Mol Genet 2000;9:249–58. [PubMed: 10607835]

Srivastava D, Cserjesi P, Olson EN. A subclass of bHLH proteins required for cardiac morphogenesis. Science 1995;270:1995–9. [PubMed: 8533092]

Stein GS, Lian JB, van Wijnen AJ, Stein JL, Montecino M, Javed A, Zaidi SK, Young DW, Choi JY, Pockwinse SM. Runx2 control of organization, assembly and activity of the regulatory machinery for skeletal gene expression. Oncogene 2004;23:4315–29. [PubMed: 15156188]

Stricker S, Fundele R, Vortkamp A, Mundlos S. Role of Runx genes in chondrocyte differentiation. Dev Biol 2002;245:95–108. [PubMed: 11969258]

Tapadia MD, Cordero DR, Helms JA. It's all in your head: new insights into craniofacial development and deformation. J Anat 2005;207:461–77. [PubMed: 16313388]

Thomas T, Kurihara H, Yamagishi H, Kurihara Y, Yazaki Y, Olson EN, Srivastava D. A signaling cascade involving endothelin-1, dHAND and msx1 regulates development of neural-crest-derived branchial arch mesenchyme. Development 1998;125:3005–14. [PubMed: 9671575]

Trokovic N, Trokovic R, Mai P, Partanen J. Fgfr1 regulates patterning of the pharyngeal region. Genes Dev 2003;17:141–53. [PubMed: 12514106]

Trumpp A, Depew MJ, Rubenstein JL, Bishop JM, Martin GR. Cre-mediated gene inactivation demonstrates that FGF8 is required for cell survival and patterning of the first branchial arch. Genes Dev 1999;13:3136–48. [PubMed: 10601039]

Tucker AS, Lumsden A. Neural crest cells provide species-specific patterning information in the developing branchial skeleton. Evol Dev 2004;6:32–40. [PubMed: 15108816]

Valverde-Franco G, Liu H, Davidson D, Chai S, Valderrama-Carvajal H, Goltzman D, Ornitz DM, Henderson JE. Defective bone mineralization and osteopenia in young adult FGFR3−/− mice. Hum Mol Genet 2004;13:271–84. [PubMed: 14681299]

Velonis, D.; Kronenberg, M.; Oliver, B.; Lichtler, A.; Mina, M. Generation of constructs expressing mutated forms of FGFR3 and mandibular morphogenesis.. Proceedings of the 56th Meeting of Hellenic Society of Biochemistry & Molecular Biology.; Larissa. Greece.. 2004. p. 135-140.

Vortkamp A, Lee K, Lanske B, Segre GV, Kronenberg HM, Tabin CJ. Regulation of rate of cartilage differentiation by Indian hedgehog and PTH-related protein. Science 1996;273:613–22. [PubMed: 8662546]

Walshe J, Mason I. Fgf signalling is required for formation of cartilage in the head. Dev Biol 2003;264:522–36. [PubMed: 14651935]

Wang YH, Upholt WB, Sharpe PT, Kollar EJ, Mina M. Odontogenic epithelium induces similar molecular responses in chick and mouse mandibular mesenchyme. Dev Dyn 1998;213:386–97. [PubMed: 9853960]

Wilke TA, Gubbels S, Schwartz J, Richman JM. Expression of fibroblast growth factor receptors (FGFR1, FGFR2, FGFR3) in the developing head and face. Dev Dyn 1997;210:41–52. [PubMed: 9286594]

Wilson J, Tucker AS. Fgf and Bmp signals repress the expression of Bapx1 in the mandibular mesenchyme and control the position of the developing jaw joint. Dev Biol 2004;266:138–50. [PubMed: 14729484]

Yu K, Xu J, Liu Z, Sosic D, Shao J, Olson EN, Towler DA, Ornitz DM. Conditional inactivation of FGF receptor 2 reveals an essential role for FGF signaling in the regulation of osteoblast function and bone growth. Development 2003;130:3063–74. [PubMed: 12756187]

Zhang X, Ibrahimi OA, Olsen SK, Umemori H, Mohammadi M, Ornitz DM. Receptor specificity of the fibroblast growth factor family. The complete mammalian FGF family. J Biol Chem 2006;281:15694–700. [PubMed: 16597617]

Zhou YX, Xu X, Chen L, Li C, Brodie SG, Deng CX. A Pro250Arg substitution in mouse Fgfr1 causes increased expression of Cbfa1 and premature fusion of calvarial sutures. Hum Mol Genet 2000;9:2001–8. [PubMed: 10942429]

Zimmermann B, Thies M. Alterations of lectin binding during chondrogenesis of mouse limb buds. Histochemistry 1984;81:353–61. [PubMed: 6511488]

Supplementary Material

Refer to Web version on PubMed Central for supplementary material.

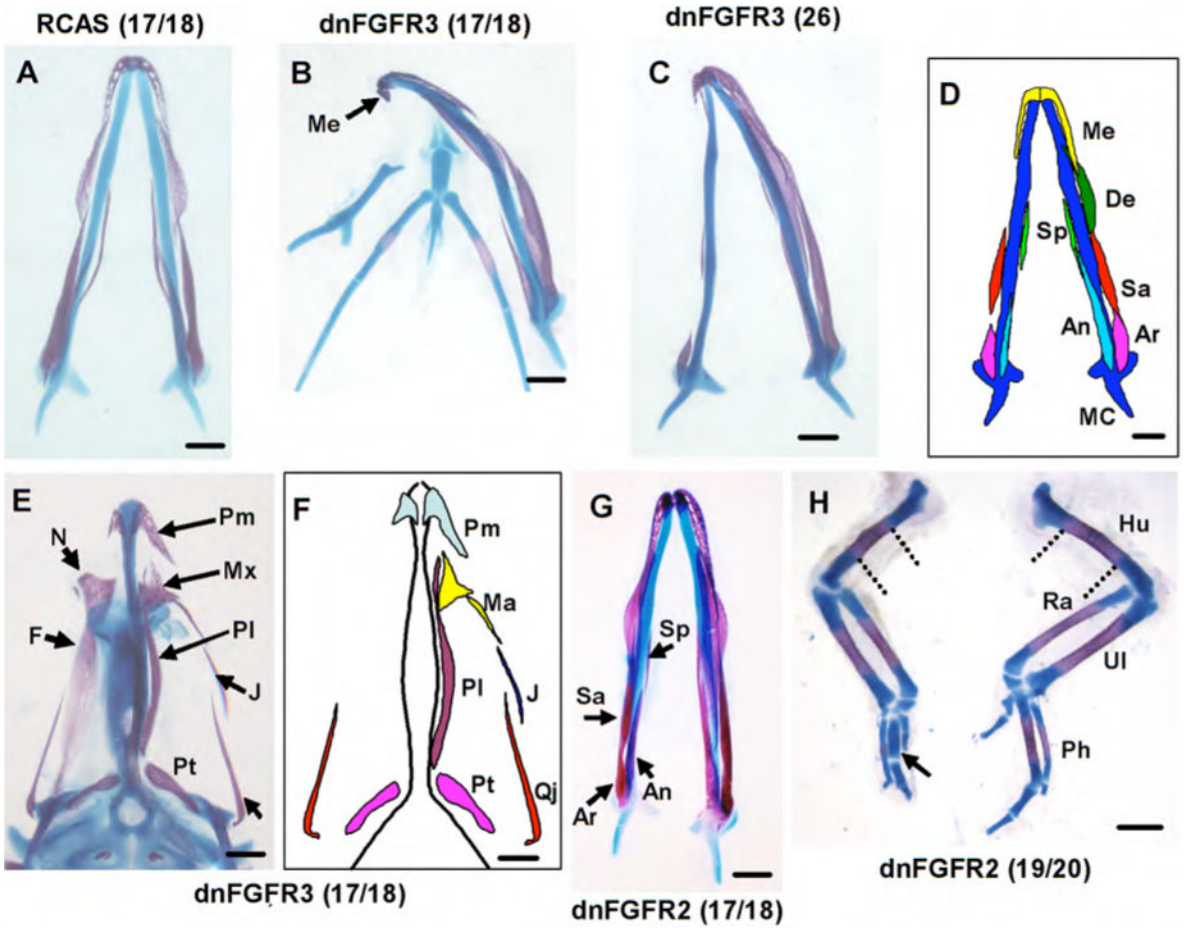

Figure 1. Effects of over-expression of dnFGFR3 and dnFGFR2 on skeletal development

(A-D) Whole-mount skeletal preparation of mandibles at HH37 after injection of control virus (A), or RCAS-dnFGFR3 (B-D) into the right mandibular process at HH17/18 (B) or HH26 (C, D). In all pictures, the injected side is on the left.

(A) A mandible injected with control virus at HH17/18, showing that skeletogenesis on the injected side of the mandible is indistinguishable from the uninjected side. (B) A mandible injected with dnFGFR3 at HH17/18 showing severe truncation of Meckel's cartilage, absence of five mandibular bones and the formation of a smaller mentomandibular bone (Me) on the injected side. Also note the alterations in the position and shape of the elements in the articulating end of the Meckel's cartilage on the injected side. (C) A mandible injected with dnFGFR3 at HH26 showing the absence of the angular, splenial, and dentary bones and the formation of smaller articular, supra-angular, and mentomandibular bones. (D) Schematic drawing illustrating the effects of dnFGFR3 injected at HH26 on the developing bones.

(E) Inferior view of a skeletal preparation of a head at HH37 after injection of RCAS-dnFGFR3 into the maxillary process at HH17/18. The mandible has been removed and the injected side is on the left of the picture. On the injected side, the maxillary, palatal and jugal bones are absent. The premaxillary, quadratojugal and pterygoid bones are smaller than those on the uninjected side. The frontal and nasal bones were unaffected and were lost on the uninjected side during dissection. (F) Schematic drawing illustrating the effects of the dnFGFR3 on the upper beak shown in E.

(G) A mandible injected with dnFGFR2 at HH17/18 showing the lack of severe defects in the developing Meckel's cartilage and smaller articular, angular, supra-angular, and splenial bones.

(H) Skeletal preparation at HH37 of the forelimb injected with RCAS-dnFGFR2 at HH19−20 (left) and the contra-lateral uninjected limb (right) from the same embryo. Note the shortening of the injected limb as compared to the uninjected limb. Also note the shortening of the humerus, radius, ulna, and phalanges, shortened ossified regions stained with Alizarin red of the humerus (indicated by dashed lines), radius, and ulna, and a lack of ossification in most phalanges (indicated by arrow) in the injected limb. Scale bars in all pictures=1mm An=angular, Ar=articular, De=dentary, F=frontal, Hu=humerus, J=jugal, MC=Meckel's cartilage, Me=mentomandibular, Mx=maxillary, N=nasal bone, Ph=phalanges, Pl=palatal, Pm=premaxillary, Pt=Pterygoid, Qi=quadratojugal, Ra=radius, Sa= supra-angular, Sp= splenial, and Ul=ulna.

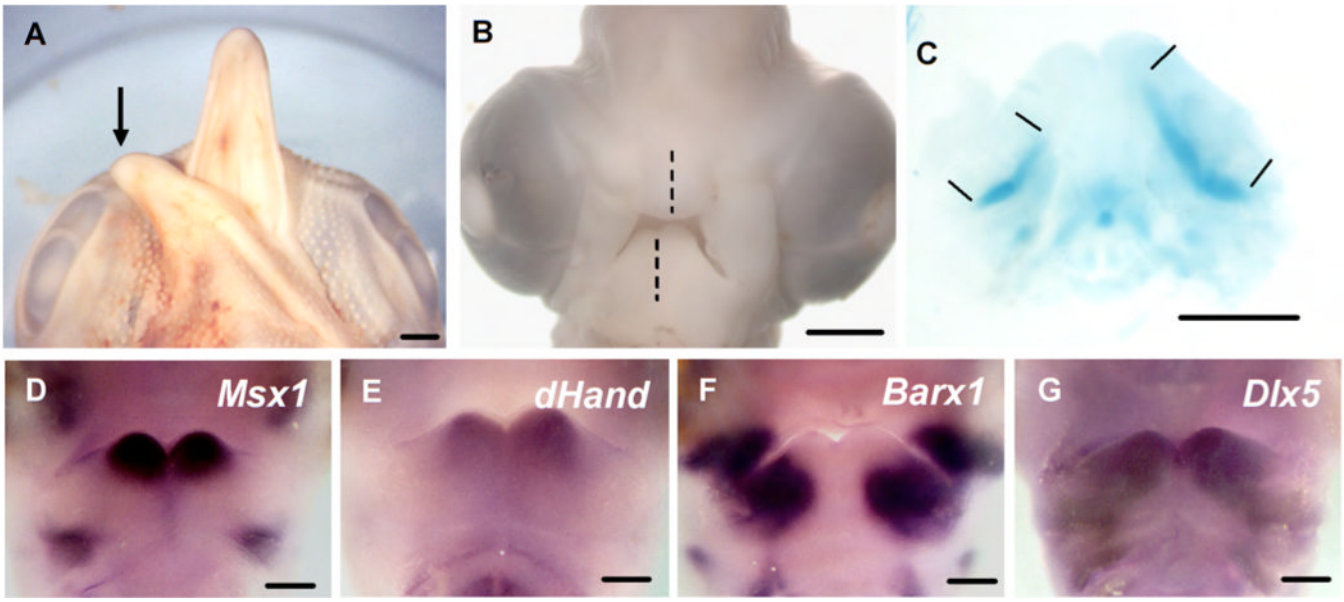

Figure 2. Effects of dnFGFR3 on mandibular outgrowth, initial formation of MC and on the expression of transcription factors in the developing mandible

(A) Inferior view of a chicken head at HH37 injected with RCAS-dnFGFR3 at HH17/18. (B) Frontal view of a chicken head at HH28−29 injected with RCAS-dnFGFR3 at HH17/18. (C) Alcian blue preparation of the mandible from the embryo in B. The injected sides of the mandible are on the left. Note the severe deviation of the mandible (indicated by arrow) towards the injected side at HH37 (8 days after injection). Also note the detectable deviation in the midline of the lower jaw from the upper jaw (indicated by dashed lines in B) and the reduced length of Meckel's cartilage (C) on the injected side. Scale bars=1mm

D-G are frontal views of whole-mount *in situ* hybridization analysis for *Msx1* (D), *dHand* (E), *Barx1* (F), and *Dlx5* (G) in the mandibular processes two days after injection of RCAS-dnFGFR3 at HH17/18. In all pictures, the injected side of the mandible is on the left. There are no detectable changes in the domains and levels of expression of these transcription factors on the injected sides of the mandible compared to the uninjected sides. Scale bars=500 μm

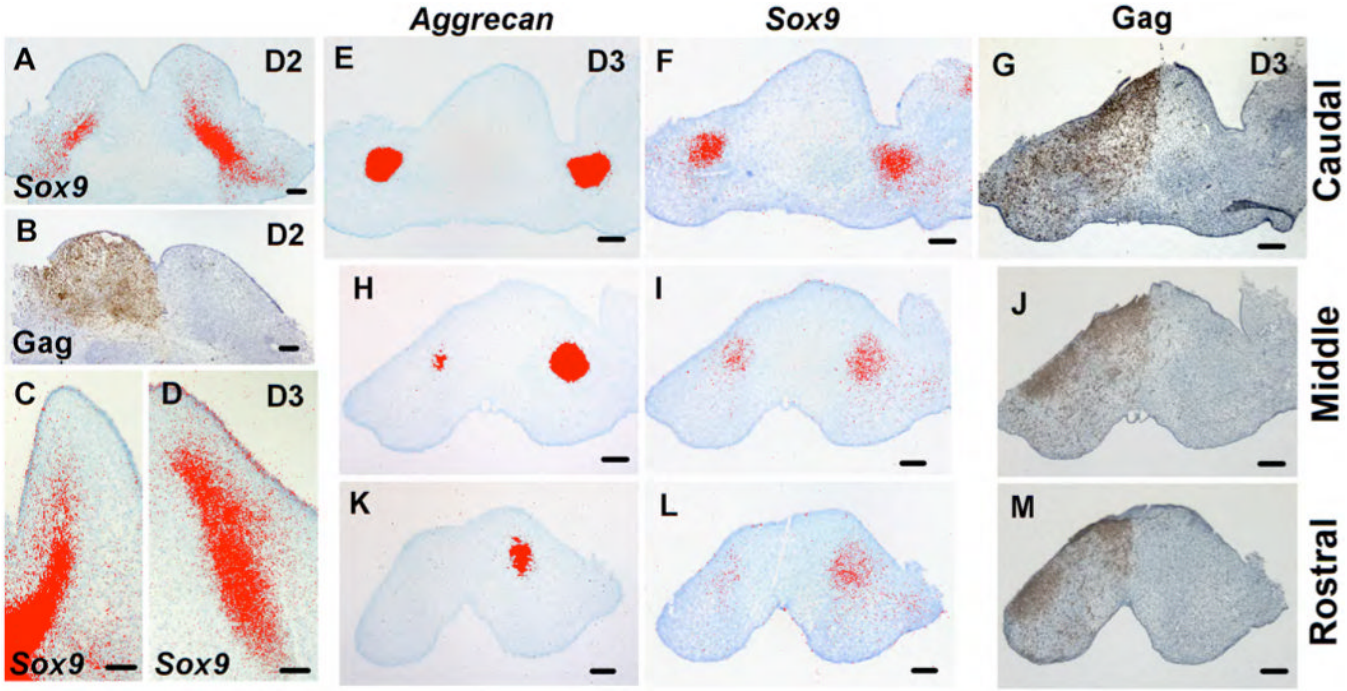

Figure 3. Effects of dnFGFR3 on the expression of markers of chondrogenesis in Meckel's cartilage

Pseudo colored images of *in situ* hybridization of *Sox9* (A, C, D, F, I, L) and *Aggrecan* (E, H, K) and immunohistochemical detection of Gag (B, G, J, M) on sections from the developing mandible two (A, B) and three (C-M) days after injection of dnFGFR3 into the right half of the developing mandible at HH17/18. In all pictures the injected side of the mandible is on the left.

(A) Sagittal section through a mandible two days after injection showing the reductions in the domain of expression of *Sox9* on the injected side. B is a sagittal section incubated with antibody to Gag showing the extensive expression of Gag in the mesenchyme on the injected side.

(C & D) Sagittal sections through mandibles three days after injection showing the reductions in the domain of expression of *Sox9* on the injected side (C) as compared to the uninjected side (D).

(E-G) are adjacent cross sections through the caudal region of the mandible showing the unchanged patterns of expression of *Aggrecan* (E) and *Sox9* (F) in Meckel's cartilage on the injected sides. The expression of Gag is shown in an adjacent section (G).

(H-J) are adjacent cross sections through the middle region of the mandible showing decreases in the domains and levels of expression of *Aggrecan* (F) and *Sox9* (G) in Meckel's cartilage in the injected sides. (J) is an adjacent section processed for immunohistochemistry with Gag antibody.

K-M are adjacent cross sections through the rostral region of the mandible showing the lack of expression of *Aggrecan* (K) and decreases in the domain and level of *Sox9* (L) in Meckel's cartilage on the injected side. M is an adjacent section processed for immunohistochemistry with Gag antibody. Scale bars in all pictures=100 μm.

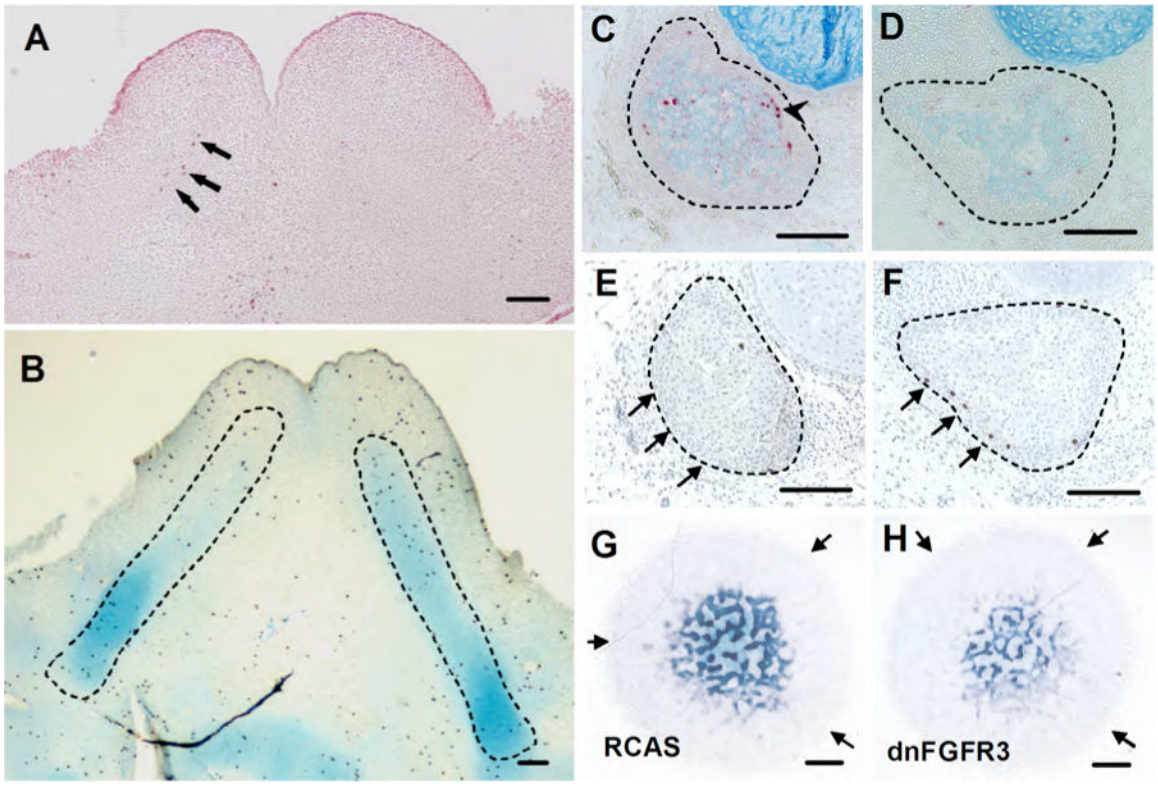

Figure 4. Effects of dnFGFR3 on the distribution of proliferative and apoptotic cells in mandibular mesenchyme and *in vitro* chondrogenesis

In all pictures the injected side of the mandible is on the left. (A) is a sagittal section through a mandible two days after injection of RCAS-dnFGFR3 at HH17/18 processed for TUNEL staining. Note the increased number of apoptotic cells in the area of the chondrogenic condensation (indicated by arrows) on the injected side. B is a sagittal section through a mandible three days after injection of RCAS-dnFGFR3 at HH17/18 processed for immunohistochemistry with an H3-p antibody. Note the decreased number of proliferative cells in the newly formed MC (outlined by dashed lines) on the injected side.

(C-F) are adjacent cross sections through the angular bone (outlined by dashed lines) six days after injection of RCAS-dnFGFR3 at HH26 processed for TUNEL staining (C and D) and immunohistochemistry with an H3-p antibody (E and F). Note the increases in the number of apoptotic cells in osteoblasts and periosteum (indicated by arrowhead) on the injected side (C) as compared to the uninjected side (D). Also note the reduced number of proliferative cells in the periosteum (indicated by arrows) on the injected side (E) as compared to the uninjected side (F). Sections B, C, and D were counterstained with Alcian blue to identify Meckel's cartilage. Scale bars in A-F= 200μm.

(G & H) are micromass cultures infected for four days with control virus (G) or RCAS-dnFGFR3 (H). Cultures were processed for Alcian blue and hematoxylin staining. Note the decreases in Alcian blue staining in cultures infected with RCAS-dnFGFR3 (H) compared to cultures infected with control virus (G). The arrows outline the periphery of the micromass cultures stained with hematoxylin. Scale bars in G and H=1 mm

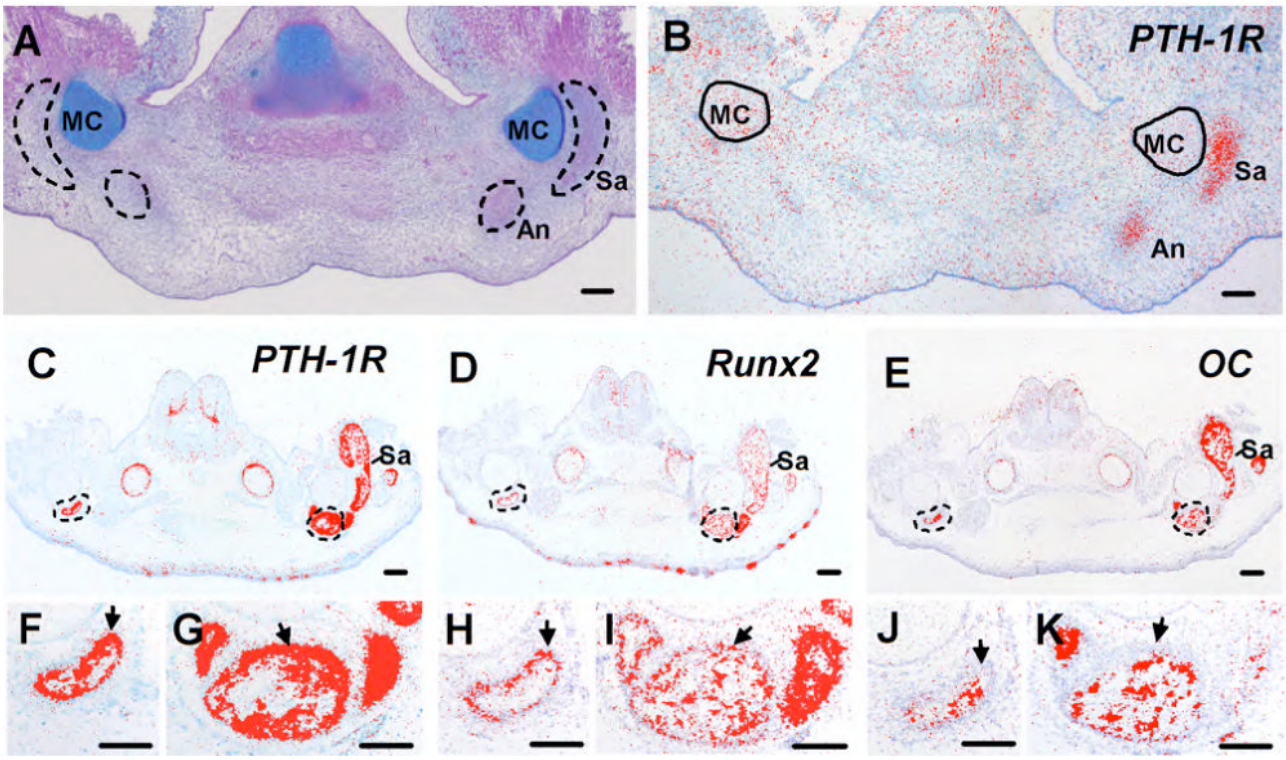

Figure 5. Effects of dnFGFR3 on osteogenic condensations and expression of markers of osteogenesis in the mandibular bones

In both pictures, the injected side of the mandible is on the left. (A & B) are adjacent cross sections through the caudal region of the mandibular process at HH31 after injection of RCAS-dnFGFR3 at HH17/18. Note the absence of morphologically recognizable osteogenic condensations (outlined by dashed lines) for the supra-angular and angular bones adjacent to Meckel's cartilage on the injected side of the mandible. (B) Pseudo-colored image of *in situ* hybridization showing expression of *PTH-1R* in the osteogenic condensations of the supra-angular and angular bones on the uninjected side. *PTH-1R* is not detected on the injected side. Scale bars= 200μm.

(C-K) Pseudo-colored images of *in situ* hybridization for *PTH-1R* (C, F, G), *Runx2* (D, H, I) and *OC* (E, J, K) in the angular bone (outlined by dashed lines) in adjacent cross sections through the caudal region of mandible 6 days after injection of RCAS-dnFGFR3 at HH26. The injected sides of the mandible are on the left. The domains of expression of *PTH-1R* (C), *Runx2* (D) and *OC* (E) in the angular bones on the injected sides of the mandible are smaller than those on the uninjected sides. Also note the absence of the supra-angular bone on the injected sides.

Figures F-K are higher magnification images of the angular bone on the injected (F, H, J) and uninjected (G, I, K) sides. Note the marked reduction in the number of *PTH-1R* and *OC* expressing osteoblasts in the angular bones on the injected sides as compared to the uninjected sides. *Runx2* is expressed in osteoblasts on the uninjected side (I), but not on the injected side (H). *PTH-1R* and *Runx2* are expressed in the periosteum (indicated by arrows) on the injected and uninjected sides.An=Angular, MC= Meckel's cartilage, and Sa=Supra-angular. Scale bars=200μm.

Table 1

Changes in the mandibular bones after injection of RCAS-dnFGFR3 and RCAS-dnFGFR2.

Construct	Stage injected	Articular		Angular		Supra-angular		Dentary		Splenial		Mento-mandibular	
		S	A	S	A	S	A	S	A	S	A	S	A
dnFGFR3	**17–20** (n-26)	27	73	19	81	12	88	23	77	4	96	88	4
	26 (n=16)	100	0	94	6	94	6	75	25	44	56	81	0
dnFGFR2	**17–20** (n=24)	92	0	79	0	79	0	0	0	79	0	0	0

Percentage of various abnormalities in the mandibular bones in HH37 embryos following injections of RCAS-dnFGFR3 or RCAS-dnFGFR2 at various stages of development.

S denotes the percentage of bones that were smaller. A denotes the percentage of bones that were absent. The six mandibular bones are arranged in a general caudal to rostral order from left to right.

Table 2

Quantitative analysis of the effects of dnFGFR3 on proliferation and apoptosis during chondrogenesis of Meckel's cartilage and osteogenesis of supra-angular and angular bones.

Stage of injection	Region of analysis	Time of analysis (days after injection)	H3-p positive (cells/mm^2)		TUNEL positive (cells/mm^2)	
			Injected	Uninjected	Injected	Uninjected
HH17/18	Mandibular mesenchyme	2	308.0 ± 6.8	307.0 ± 8.4	65.5 ± 7.6 *	29.7 ± 2.0
HH17/18	Newly formed Meckel's cartilage	3	143.3 ± 9.3*	283.7 ± 17.9	174.6 ± 10.1*	41.6 ± 6.7
HH17/18	Rostral third of Meckel's cartilage	4	287.4 ± 26.3	341.7 ± 21.1*	0	0
HH17/18	Middle third of Meckel's cartilage	4	246.4 ± 18.7	221.4 ± 12.1	0	0
HH17/18	Caudal third of Meckel's cartilage	4	253.9 ± 19.1	249.9 ± 13.2	0	0
HH17/18	Osteogenic condensation for supra-angular bone	4	27.3 ± 1.5	55.6 ± 1.9	24.8 ± 3.9	13.9 ± 2.1
HH26	Differentiated angular bone	6	88.0 ± 7.8*	115.4 ± 7.2	122.2 ± 15.8*	72 ± 7.6

Quantification of H3-p positive cells and TUNEL positive cells was performed as described in Materials and Methods. The areas for quantitative analysis included the entire area of the mandibular mesenchyme (shown in 4A), newly formed cartilage (outlined in Figure 4B), osteogenic condensation for supra-angular bone (outlined in Figure 5A) and differentiated angular bone (outlined in Figures 4 C-F and 5 C-E). All values represent means ± SE of proliferative and apoptotic cells/mm^2 in 6−17 sections (described in Materials and Methods) in 4 independent experiments. ND, not determined. Asterisks indicate a statistically significant difference ($p<0.01$).

Table 3

Quantification of the effects dnFGFR3 on *in vitro* chondrogenesis of mandibular mesenchyme.

Analysis	Days	RCAS	RCAS-dnFGFR3	RCAS-dnFGFR2
# of aggregates	2	134.3 ± 17.3 (n=6)	111 ± 5.5 (n=6)	ND
Size of aggregates (mm^2)	2	0.05 ± 0.009 (n=6)	0.045 ± 0.005 (n=6)	ND
Relative absorbance	4	117.9 ± 6.3 (n=16)	73.8 ± 2.0* (n=12)	105.8 ± 4.5 (n=12)
	6	160.0 ± 6.1 (n=16)	88.2 ± 8.7* (n=12)	146.3 ± 8.2 (n=12)
Relative area stained by Alcian blue	4	8.46 ± 0.33 (n=16)	5.53 ± 0.14* (n=12)	7.87 ± 0.24 (n=12)
	6	10.67 ± 0.27 (n=16)	6.24 ± 0.69* (n=12)	10.18 ± 0.67 (n=12)
PNA/Alcian blue	3	1.07 + 0.01 (n=13)	1.18 + 0.02* (n=11)	ND
	4	1.12 + 0.02 (n=10)	1.25 + 0.11* (n=10)	ND

The quantification of various parameters was determined as described in the Materials and Methods. Values represent the mean ± S.E. for 6−12 cultures (indicated in parenthesis) in two or three independent experiments. ND, not determined. Asterisks indicate statistical significance at $p<0.01$.